

# A Ka-Band Wide-Bandgap Solid-State Power Amplifier: Architecture Performance Estimates

P. Khan,<sup>1</sup> L. Epp,<sup>1</sup> and A. Silva<sup>1</sup>

Motivated by recent advances in wide-bandgap (WBG) gallium nitride (GaN) semiconductor technology, there is considerable interest in developing efficient solid-state power amplifiers (SSPAs) as an alternative to the traveling-wave tube amplifier (TWTA) for space applications. This article documents the results of a study to investigate power-combining technology and SSPA architectures that can enable a 120-W, 40 percent power-added efficiency (PAE) SSPA. Results of the study indicate that architectures based on at least three power combiner designs are likely to enable the target SSPA. The proposed architectures can power combine 16 to 32 individual monolithic microwave integrated circuits (MMICs) with >80 percent combining efficiency. This corresponds to MMIC requirements of 5- to 10-W output power and >48 percent PAE. For the three proposed architectures [1], detailed analysis and design of the power combiner are presented.

The first architecture studied is based on a 16-way septum combiner that offers low loss and high isolation over the design band of 31 to 36 GHz. Analysis of a 2-way prototype septum combiner had an input match >25 dB, output match >30 dB, insertion loss <0.02 dB, and isolation >30 dB over the design band. A 16-way design, based on cascading this combiner in a binary fashion, is documented. The second architecture is based on a 24-way waveguide radial combiner. A prototype 24-way radial base was analyzed to have an input match >30 dB (under equal excitation of all input ports). The match of the mode transducer that forms the output of a radial combiner was found to be >27 dB. The functional bandwidth of the radial base and mode transducer, which together will form a radial combiner/divider, exceeded the design band. The third architecture employs a 32-way, parallel-plate radial combiner. Simulation results indicated an input match >24 dB, output match >22 dB, insertion loss <0.23 dB, and adjacent port isolation >20 dB over the design band. All three architectures utilize a low-loss MMIC amplifier module based on commercial MMIC packaging and a custom microstrip-to-rectangular-waveguide transition. The insertion loss of the module is expected to be 0.45 dB over the design band.

---

<sup>1</sup> Communications Ground Systems Section.

This research was carried out at the Jet Propulsion Laboratory, California Institute of Technology, and was sponsored by Glenn Research Center, and the National Aeronautics and Space Administration. Reference herein to any specific commercial product, process, or service by trade name, trademark, manufacturer or otherwise, does not constitute or imply its endorsement by the United States Government or the Jet Propulsion Laboratory, California Institute of Technology.

## I. Introduction

This article presents results of a study to evaluate several solid-state power amplifier (SSPA) architectures and survey the underlying wide-bandgap (WBG) monolithic microwave integrated circuit (MMIC) technology. The goal is to assess whether expected advances in WBG technology can make a solid-state replacement of a traveling-wave tube amplifier (TWTA) feasible. The program goals and general SSPA architecture issues are summarized in a previous article [2]. In this article, detailed analyses of three SSPA architectures are presented. Based on these results, the desired MMIC characteristics are determined and compared with the current performance and expected improvements in WBG technology.

## II. WBG SSPA Architectures

To power combine a large number of devices in the SSPA with good efficiency, a combining circuit is required that has minimum power loss and adequate port-to-port isolation. Planar combining circuits such as branchline and Wilkinson couplers provide good isolation between combining ports. However, as discussed in [2], loss of planar transmission lines at 32 GHz (Ka-band) are prohibitive for efficient power combining. Such circuits implemented in waveguide have significantly lower loss, but generally have mass and bandwidth limitations.

The previous survey of low-loss, millimeter-wave power combining techniques [1] determined that power combiners demonstrated to date do not meet all of the requirements of the current application. Therefore, detailed analysis of three custom power combiner designs was undertaken in the subsequent phase of this study. These designs were chosen to provide different numbers of combining ports (16, 24, and 32) such that a range of MMICs potentially can be integrated to implement the target SSPA. In the SSPA architectures discussed below, the power combiner is also used as the input power divider, with layout changes if required. This results in a simplified architecture that is easier to manufacture and potentially has greater reliability compared to the approach of using a planar divider. Should mass become a limiting factor, implementing the input divider using planar dividers potentially could reduce mass. All dividers/combiners were designed to have a waveguide interface. This allows the MMICs to be packaged in standard modules that can be integrated with any divider/combiner architecture.

The standard MMIC module is described next. In subsequent sections, the three selected power combiner designs and the associated SSPA architectures are discussed in turn.

### A. MMIC Amplifier Module

The microstrip-to-waveguide transition discussed in a previous article [2] was used to design a MMIC amplifier module with standard waveguide ports, as shown in Fig. 1. In this figure, two Stratedge SE-40 packages are shown for illustration.

The module, as shown, houses a packaged driver MMIC, a packaged power MMIC, two microstrip-to-waveguide transitions, and bias circuit boards. The module is intended to be fabricated as a split-block design with the mating surface located as indicated in the side view. The bottom half of the module would be fabricated using copper to make it an effective heat spreader. To save mass, the top half of the module would be fabricated using aluminum. It should be noted that the indicated length and width of the module can accommodate standard waveguide flanges for easy prototype development and testing. In flight implementations, a custom flange can be used to significantly reduce the lateral dimensions and hence reduce mass. The mass of the module with two MMIC packages as shown in Fig. 1 is estimated to be  $\sim$ 58 grams. The mass of a module with a single MMIC package is estimated to be  $\sim$ 46 grams.

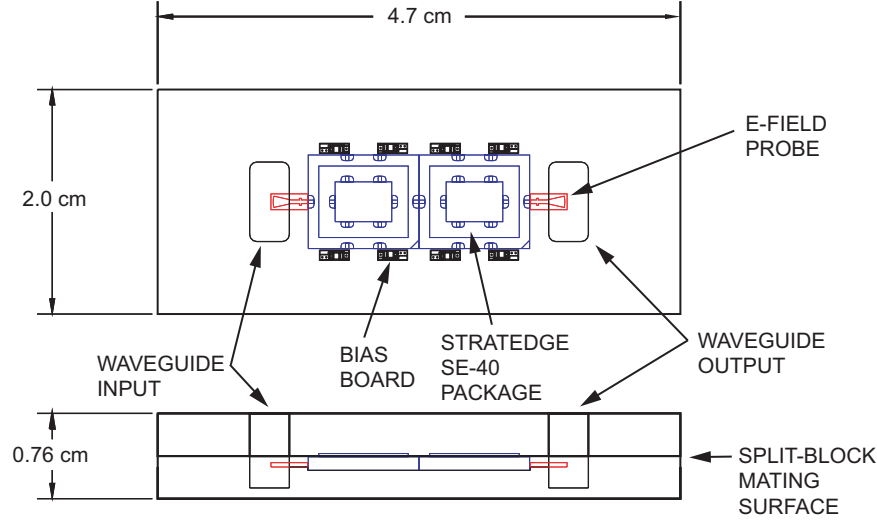


**Fig. 1. MMIC amplifier module with standard waveguide input and output.**

By standardizing on a waveguide interface, these modules can be designed, fabricated, and tested independently from the power combiners. Cost and reliability benefits can also be maximized by manufacturing and testing these modules in quantity.

All three combiners, discussed next, utilize this standard MMIC module for integrating both driver MMICs and power MMICs.

## B. Septum Combiner Architecture

**1. Thin-Film Septum Binary Combiner.** Binary, or corporate, combining is one of the most widely used combiner topologies for SSPA applications. In this approach, identical two-way combiners are cascaded in  $n$  stages to obtain a combiner with  $N = 2^n$  combining ports. Thus, once the two-way combiner (also known as an adder) is designed, it is relatively straightforward to obtain any number of combining ports that are a multiple of two. The “unit” adder generally need not be re-designed if the required SSPA power or the available MMIC power changes by a factor of two. Performing the combining in multiple stages also offers greater flexibility with respect to where gain elements can be inserted. Thus, a greater range of driver and power MMICs can be accommodated for a given application. In circumstances where the SSPA requirements have not been fixed or, as in the current case, in which specifications of the MMICs to be used have not been finalized, this flexibility at the combiner level is a distinct advantage. The fundamental drawback of the binary approach, however, is that the performance limitations of the adder are magnified by at least a factor of two for each stage of power combining. Thus, the adder loss, bandwidth, and phase balance requirements become increasingly stringent with an increasing number of combining ports.

During the power combiner survey [1], no existing adder circuits were found that meet the general requirements, are easy to manufacture at Ka-band, and potentially can meet SSPA mass limits. One approach that seemed to hold great promise is the bifurcating waveguide septum design shown in Fig. 2. In this combiner, a metal septum, oriented in the H-plane, bisects the waveguide into two reduced-height waveguides. This structure is broadband and compact, and it has extremely low-loss. However, as with any lossless three-port circuit, the combiner, as shown, does not have good port match or isolation. To improve isolation and port match, prior efforts have employed resistive cards, as in [3], or a slotted septum loaded with a discrete resistor [4]. In the first approach, as the thickness of the resistive card

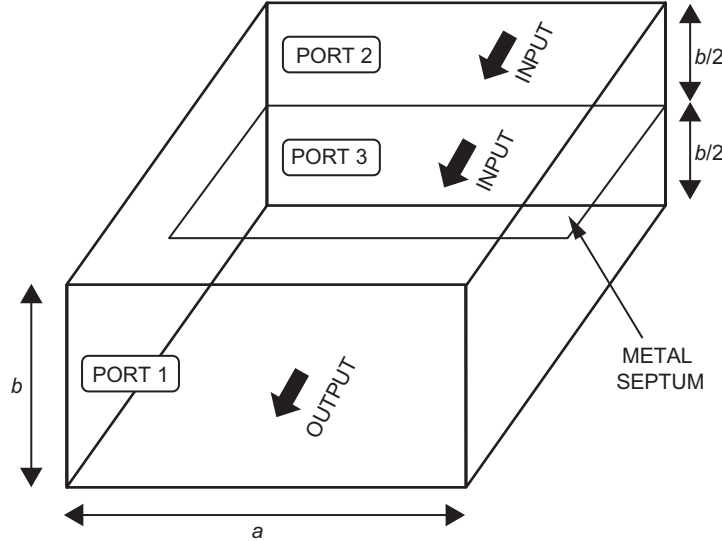


**Fig. 2. Waveguide septum combiner geometry.**

becomes greater than a skin depth at higher frequencies, the insertion loss is greatly increased. The second approach alleviates the insertion loss problem, but cannot be implemented at Ka-band due to small waveguide dimensions.

The current work has demonstrated a new resistive septum combiner, Fig. 3, with greatly improved performance over prior designs [5].<sup>2</sup> The design is relatively easy to implement at Ka-band and can be extended to higher frequencies. Unlike prior art, the resistive element of the septum is implemented using thin-film resistor technology commonly employed in hybrid microwave circuit fabrication. The resistive part of the septum consists of a low-loss dielectric substrate uniformly coated with a film of tantalum nitride (TaN) resistive material. The thickness of the film is generally on the order of a few micrometers. This approach is similar to the concept of employing a bulk resistive card. However, in the current approach, the thickness of the TaN film can be made less than a skin depth at millimeter-wave frequencies.

A balanced port excitation results in an odd-mode surface current on the resistive sheet. The component of surface current due to port 1 power effectively cancels the current due to port 2 power. No penalty in insertion loss is incurred since power loss in the resistive septum in this case is, in theory, zero. An unbalanced excitation at the input ports, however, results in an even-mode current distribution on the resistive sheet. Power in this case is absorbed by the film, as desired.

The prototype combiner in Fig. 3 is planned for fabrication and testing to demonstrate the thin-film resistive septum concept. The input full-height waveguides are matched to reduced-height waveguides formed by the bifurcation using stepped impedance transformers. Mitered E-plane bends also are included in the design for a convenient layout of the ports. An effort was made to maintain accurate symmetry about the y-z plane to ensure proper amplitude and phase balance. The septum will be implemented by stacking two 0.13-mm-thick alumina substrates. The mating surface of one substrate is designed for 128 ohms/sq. TaN film. This technique ensures accurate placement of the resistive sheet on the symmetry plane, with an equal thickness of dielectric on either side. Standard sheet resistance tolerance ( $\pm 10$  percent) was found to be adequate in the design.

---

<sup>2</sup> A. R. Khan, L. W. Epp, D. J. Hoppe, and D. Kelley, *Thin-Film Resistive Septum Waveguide Power Combiner*, JPL New Technology Report no. 40903 (internal document), Jet Propulsion Laboratory, Pasadena, California, November 16, 2004.

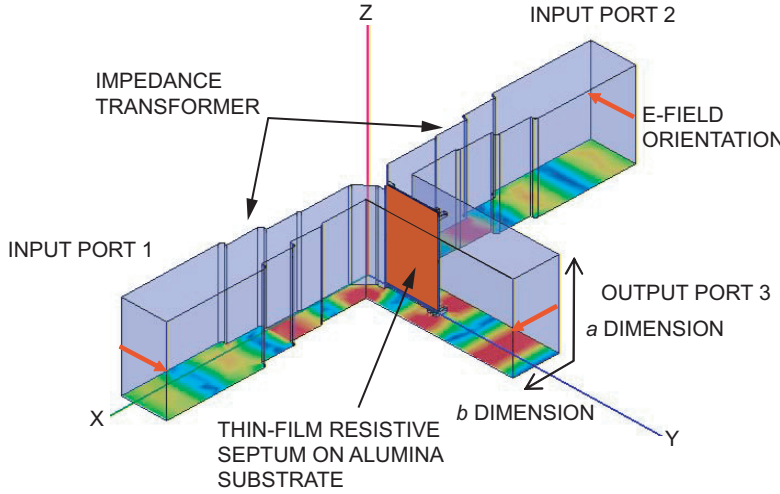


**Fig. 3. 3-D finite element model of the septum combiner. The plot of the H-field magnitude is shown on the narrow wall of the waveguide.**

The Ansoft HFSS analysis results for the two-way combining circuit are shown in Fig. 4. Excellent results were achieved over the design frequency band of 31 to 36 GHz (port match >25 dB, insertion loss <0.02 dB, isolation >30 dB). This is more than adequate for the current application.

**2. 16-Way Septum Combiner SSPA.** The septum combiner discussed above can be cascaded in a binary fashion to obtain the number of combining ports needed for the current application [6]. Figure 5 illustrates the physical architecture of an SSPA based on a 16-way combiner. In this design, the same general circuit is used as the combiner as well as the divider. As indicated in the cross section of the SSPA shown in Fig. 5(a), both the input divider and the output combiner are machined into a single waveguide layer. The divider and combiner ports couple to MMIC modules through standard waveguide interfaces. These modules are of the type discussed earlier (Fig. 1). All modules are mounted on a single baseplate for effective heat dissipation.

The plan view of the SSPA is illustrated in Fig. 5(b). The power at the input port, after being amplified by driver module 1, drives two units of driver module 2. Each driver module 2, in turn, drives 8 power amplifier modules. The outputs of all 16 power amplifier modules are combined by a 16-way septum combiner and delivered to the output port.

The radio frequency (RF) architecture of the SSPA is illustrated in Fig. 6. Two cases of gain and power level at each block are indicated above the figure. In case 1, a 41-dBm power amplifier (PA) module with 13-dB gain is used. In this case, the gain and output power of driver module 1 are 28 dB and 28 dBm, respectively, and the gain and output power of driver module 2 are 13 dB and 38 dBm, respectively. In case 2, the output power of the PA module is the same as in case 1, but the gain is reduced to 10 dB. In this case, the power and gain requirements of driver module 2 are identical to the PA module. It can be seen, however, that the gain and output power requirements of driver module 1 are increased to 34 dB and 34 dBm. In both case 1 and case 2, the 2-way divider is assumed to have zero loss, and the 8-way dividers and the 16-way combiner are assumed to have 1-dB loss each.

**3. 16-Way Septum Combiner SSPA Performance Estimates.** In summary, the performance estimates for a 160-W SSPA based on a 16-way septum combiner are given in Table 1.

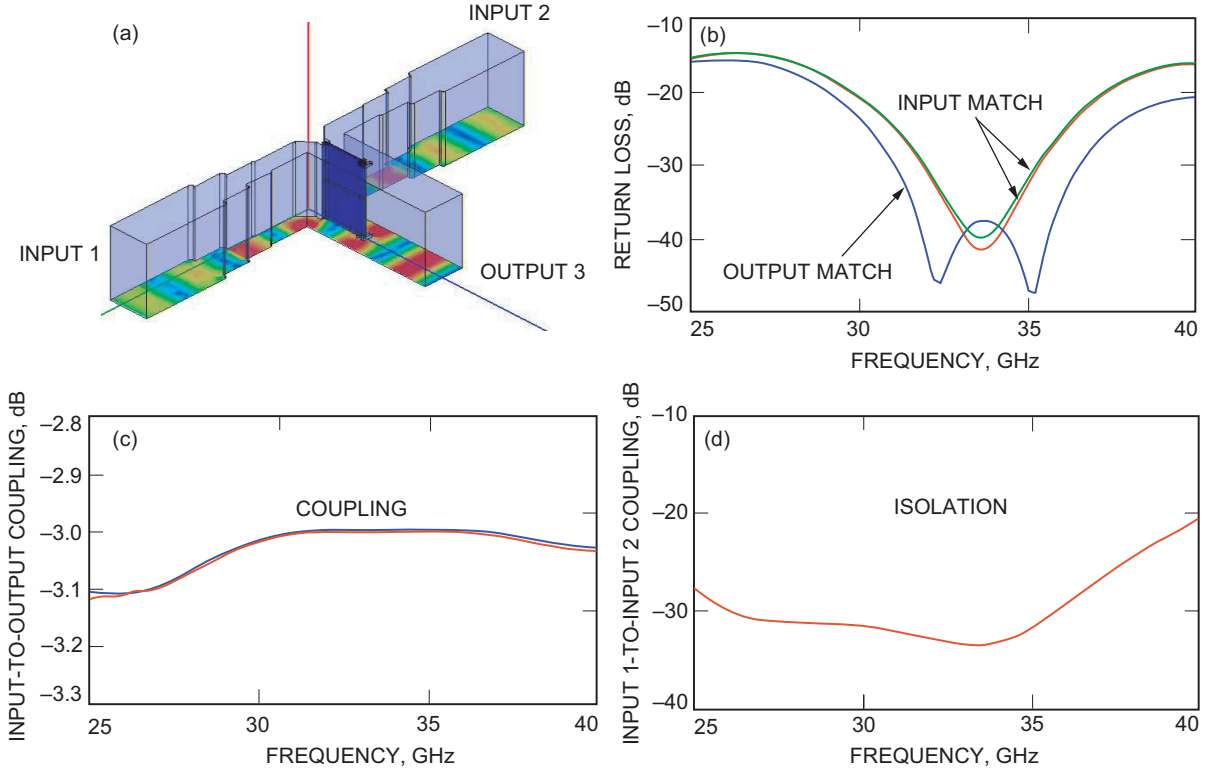


**Fig. 4. Ansoft HFSS analysis of the prototype two-way septum combiner design: (a) geometry of the septum combiner showing the output and input ports, (b) input and output match, (c) input-to-output coupling, and (d) input-to-input coupling.**

### C. Waveguide Radial Combiner Architecture

**1. Waveguide Radial Combiner.** A higher-order ( $N = 24$ ) power combining using a novel radial power combiner that exceeds 15 percent bandwidth (31 to 36 GHz) has been demonstrated; see Fig. 7 [7].<sup>3</sup>

The waveguide radial combiner consists of two parts: a mode transducer and a radial base. The radial base combines the  $N$  rectangular waveguide inputs, and outputs into a circular waveguide TE<sub>01</sub> mode; see Fig. 8.

The circular waveguide output of the radial base represents the combined power of the  $N = 24$  rectangular waveguides in a TE<sub>01</sub> circular waveguide mode. Figure 9 shows the electric field entering a WR-28 input port of the radial base, and being combined into the circular waveguide along the z-axis. Figure 10 shows that the input match for equal excitation of all rectangular input ports, as predicted by analysis, is better than 30 dB over the required band of operation.

The mode transducer then takes the circular waveguide (CWG) of the radial base and couples it back to a rectangular waveguide output. The mode transducer is a new implementation of a “Marie” transducer, which takes the TE<sub>01</sub> circular waveguide mode and converts it into the standard rectangular waveguide mode [8]. The match at both the rectangular and circular ports of JPL’s mode transducer, as determined by simulation, is shown in Fig. 11.

<sup>3</sup> L. W. Epp, A. R. Khan, D. J. Hoppe, and D. Kelley, *Wideband 24-Way Radial Power Combiner/Divider Fed by a Marie Transducer*, JPL New Technology Report no. 41511 (internal document), Jet Propulsion Laboratory, Pasadena, California, December 7, 2004.

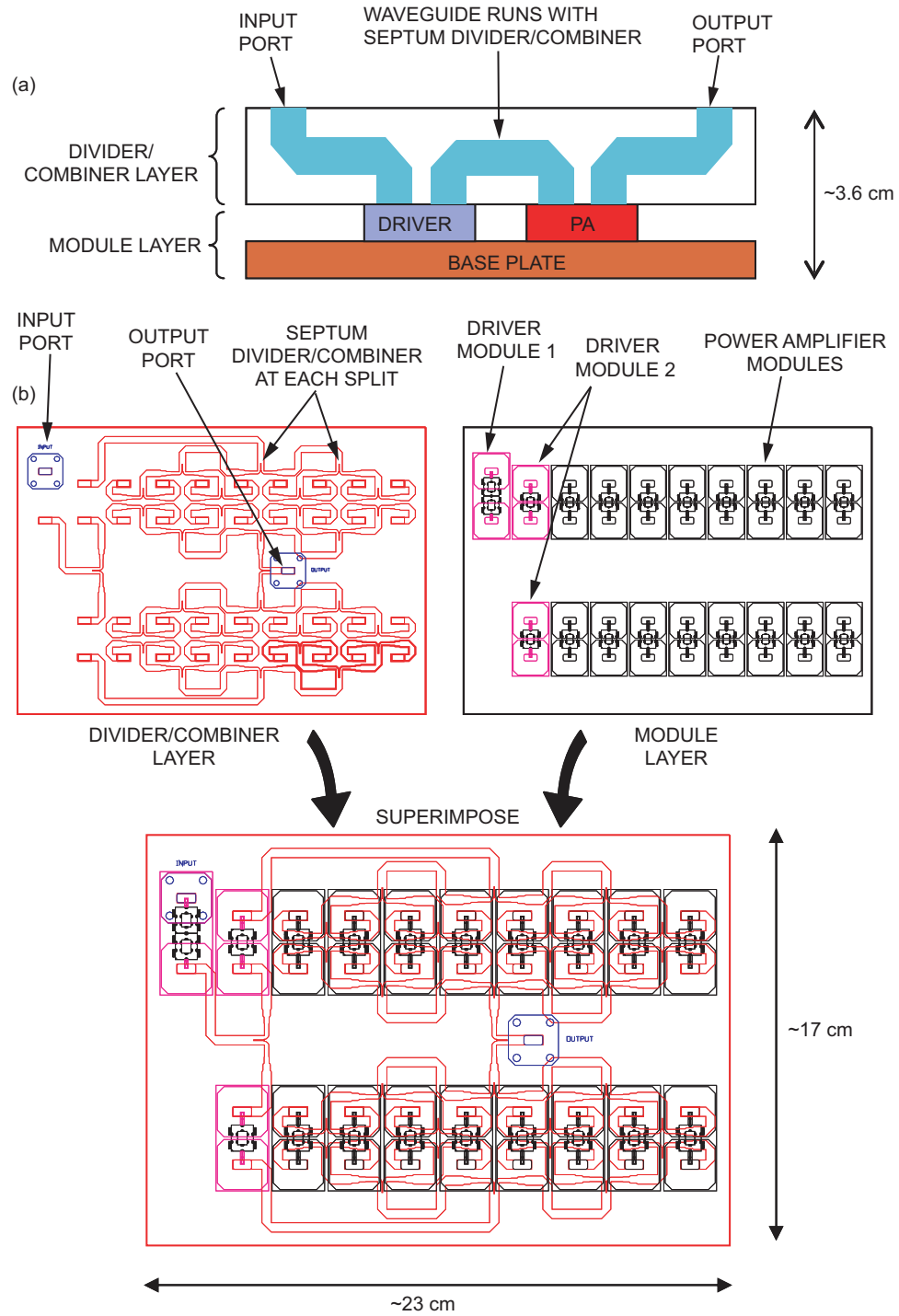


**Fig. 5.** Physical architecture of an SSPA based on a 16-way septum binary divider/combiner: (a) cross-sectional view and (b) plan view showing the layout of the power divider, power combiner, and MMIC modules.

CASE 1	POWER:	0 dBm	28 dBm	25 dBm	38 dBm	28 dBm	41 dBm	52 dBm
	GAIN:		28 dB	-3 dB	13 dB	-10 dB	13 dB	11 dB
CASE 2	POWER:	0 dBm	34 dBm	31 dBm	41 dBm	31 dBm	41 dBm	52 dBm
	GAIN:		34 dB	-3 dB	10 dB	-10 dB	10 dB	11 dB

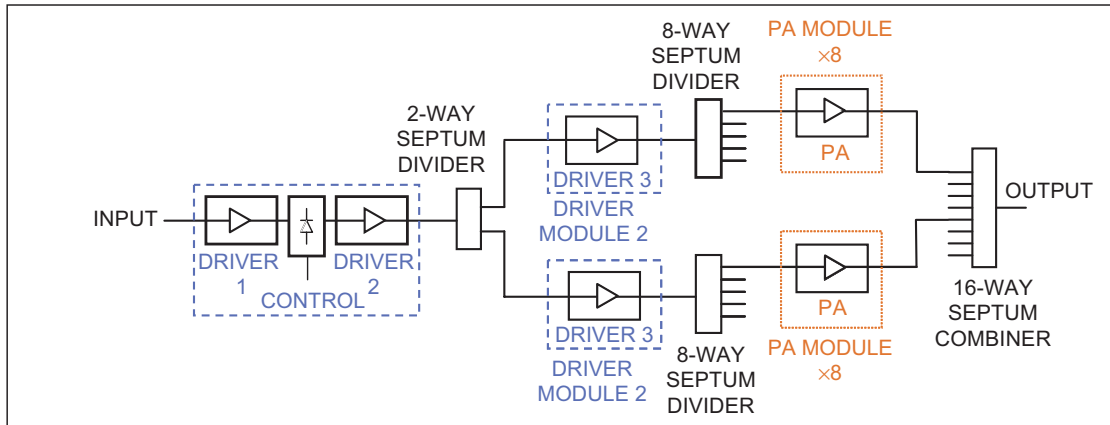


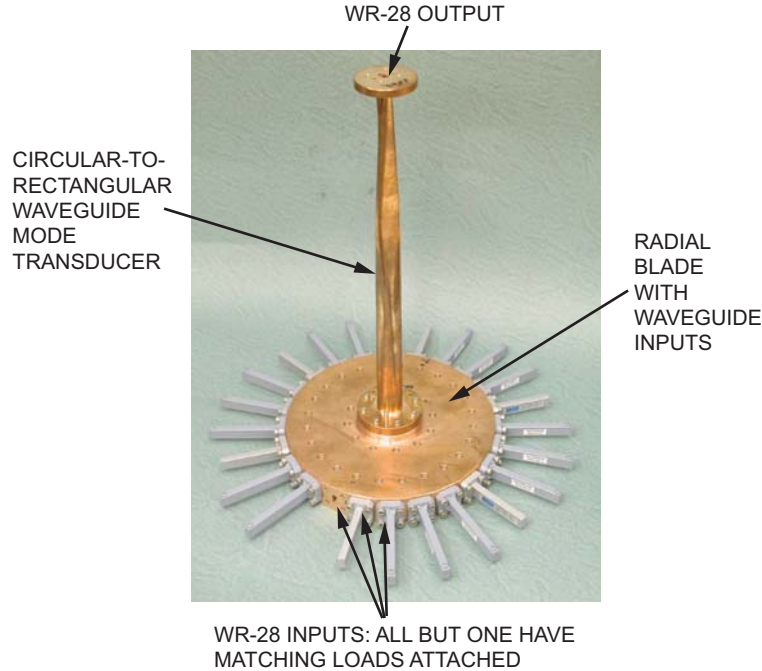
Fig. 6. RF architecture of a 52-dBm SSPA with 52-dB gain based on a 16-way septum combiner.

Table 1. 16-way septum combiner 160-W (52-dBm) SSPA estimates.

Parameter	Value
Order of combining	$N = 16$
Power combiner loss	0.34 dB
Total combining loss, including MMIC package and transition	0.89 dB (82 percent combining efficiency)
Prototype mass	3.7 kg
Prototype volume	$\sim 1400 \text{ cm}^3$
Required MMIC power	12 W
Required MMIC PAE	49 percent

A good output match at the circular waveguide of the radial base is primarily a function of the matching post in the radial base, which in turn, with a good design of the mode transducer, allows for a good output match of the combiner. For purposes of discussion, the prototype waveguide radial combiner has been described as a power combiner, but it also functions as a power divider.

**2. 24-Way Waveguide Radial Combiner SSPA.** The physical architecture of a waveguide radial-combiner-based SSPA is illustrated in Fig. 12. The combiner and the divider circuits, oriented back-to-back, are identical except for the waveguide runs that couple power to the PA modules. The driver and PA modules are mounted on a baseplate to enable effective heat removal. As illustrated, the baseplate must have a cutout to accommodate the input Marie transducer. Since loss in the input circuit is not critical, coaxial line is used to route the input signal to the power divider.



**Fig. 7. Prototype 24-way waveguide radial combiner.**

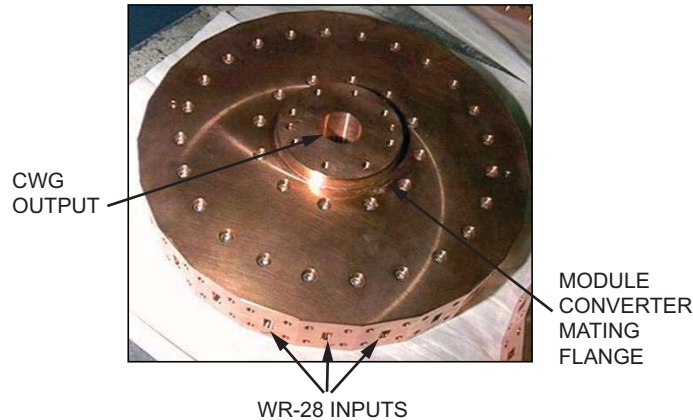


**Fig. 8. Prototype 24-way radial base.**

The diameter of the SSPA is determined by the width of the MMIC modules. The indicated 28-cm diameter (Fig. 12) is based on a full-width module that can accommodate a standard WR-28 flange. At the expense of heat density, the SSPA diameter can be reduced by decreasing the width of the MMIC modules.

The RF architecture of the waveguide radial-combiner-based SSPA is illustrated in Fig. 13. Twenty-four PA modules are power combined in a single combining stage to deliver a 52-dBm SSPA output. For the purpose of calculating the power and gain of each block, the losses of the divider and combiner circuit were assumed to be 1 dB each. A driver MMIC with sufficient gain is included in the PA module to deliver a PA module gain of 25 dB. The driver module, housing two driver MMICs and control circuits, would need to deliver 29-dBm drive power with 29-dB gain.

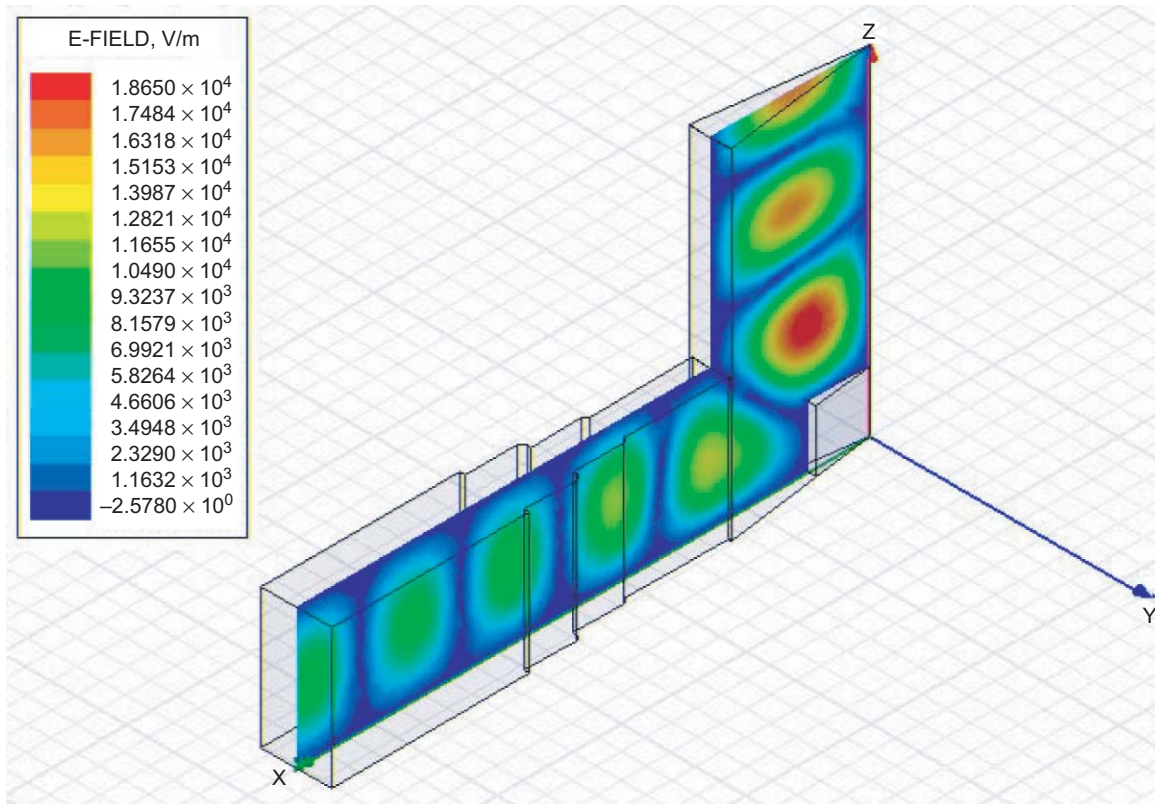


**Fig. 9.** Cross-sectional view of the radial base combining the power from the rectangular input port on the x-axis into the circular waveguide on the z-axis.

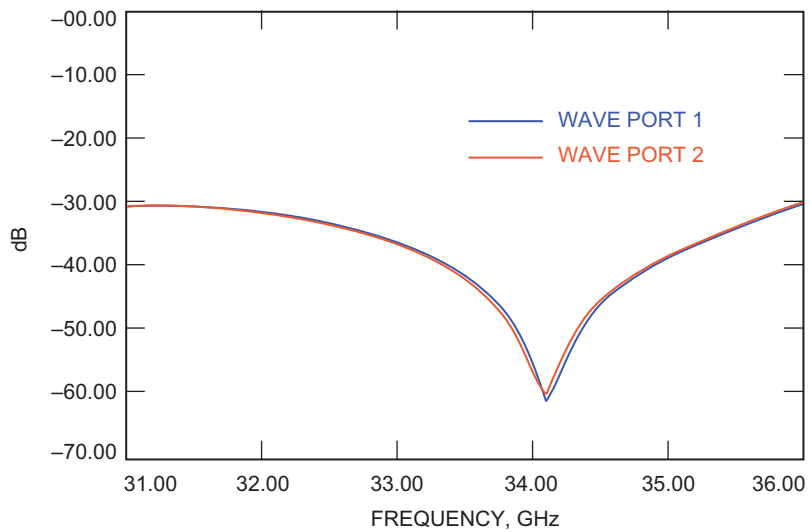


**Fig. 10.** Radial base input match at the rectangular input port (wave port 2) for equal excitation of all rectangular input ports, and at the circular waveguide port (wave port 1).

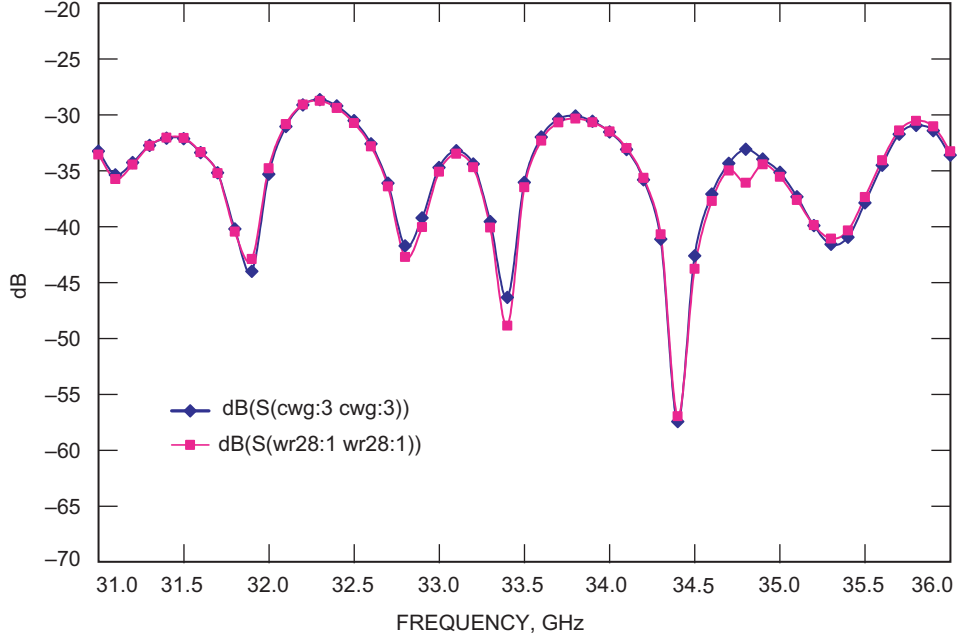


**Fig. 11.** Analytical input match at the rectangular port (wr28:1) and at the circular waveguide port (cwg:3) of JPL's Marie-mode transducer shown in Fig. 7.

**3. 24-Way Waveguide Radial Combiner SSPA Performance Estimates.** In summary, the performance estimates for a 160-W SSPA based on a 24-way waveguide radial combiner are given in Table 2.

#### D. Parallel-Plate Radial Combiner Architecture

**1. Parallel-Plate Radial Combiner.** The third combiner studied in this task is a parallel-plate radial combiner with 32 input ports. The combiner illustrated in Fig. 14 was designed for operation over the 31- to 36-GHz band [9].<sup>4</sup> There are two novel design features that are advancements over prior art. First, there is direct coupling between input rectangular waveguides and the parallel-plate guide. Unlike prior art, no dielectric matching “pills” are required [10]. This approach greatly improves manufacturability of the combiner at Ka-band and eliminates the dielectric loss of the matching element and adhesive. Second, longitudinal resistive slots are included in each plate of the parallel-plate guide to improve port match and isolation. For equal excitation at the input ports, the surface current on the plates is longitudinal. Since the slot edges in this case are at the same potential, no power couples to the resistive element. Thus, a low-loss operation is ensured. If, however, there is unequal excitation at the input ports, potential is generated across the slots and power is dissipated in the resistive element as desired. This results in good port-to-port isolation.

The power from the input ports “converges” at the center of the parallel-plate guide. There, the power is coupled through a coaxial probe to the output port. For the purpose of designing the combiner, the output port is kept coaxial. For an actual SSPA implementation, it is envisioned that the coaxial line can be coupled to a waveguide output using a conventional probe-type adaptor.

---

<sup>4</sup> A. R. Khan, L. W. Epp, and D. J. Hoppe, *Wideband (31 to 36 GHz) Parallel Plate Power Combiner/Divider with Isolation*, JPL New Technology Report no. 41758 (internal document), Jet Propulsion Laboratory, Pasadena, California, January 31, 2005.

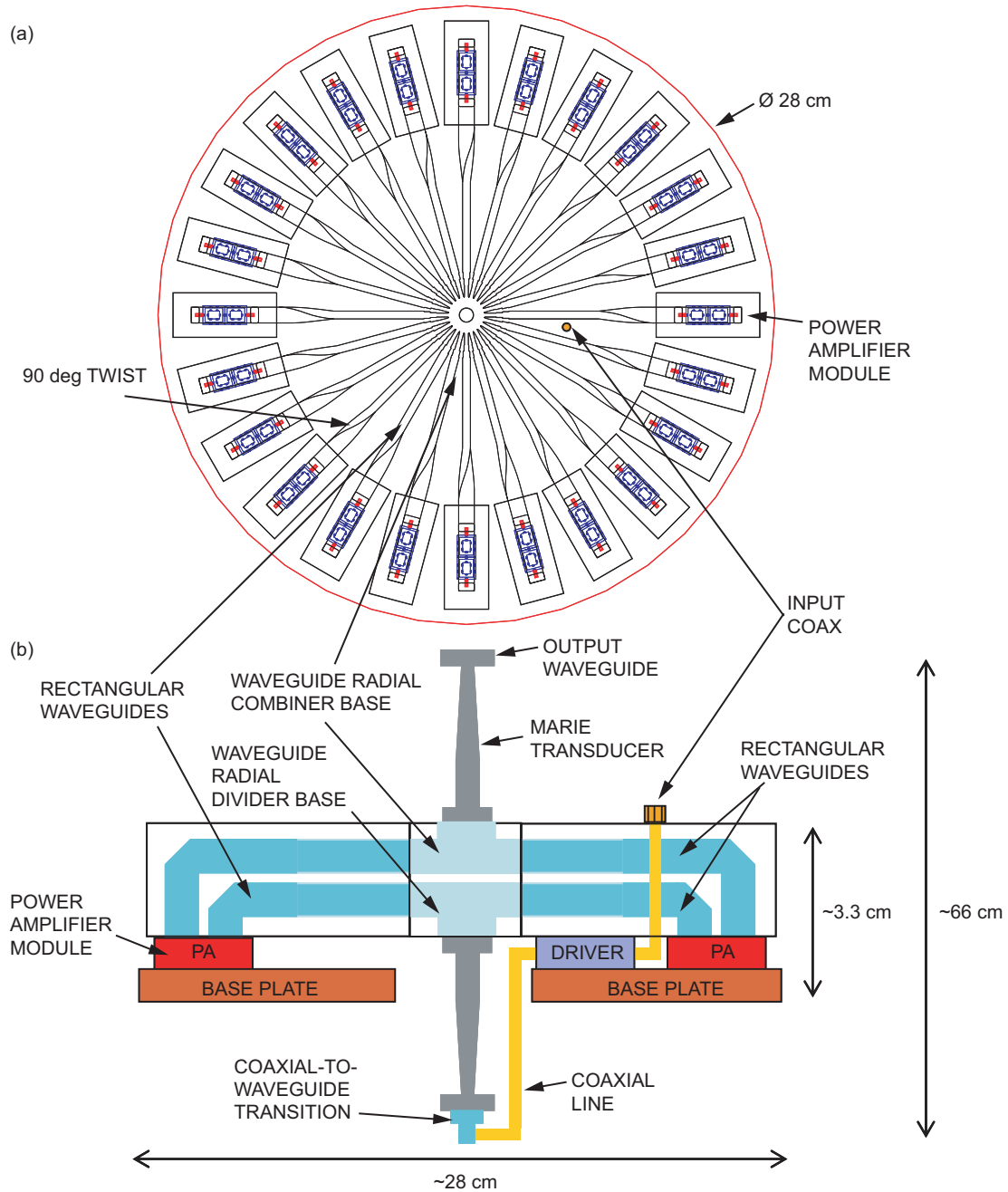
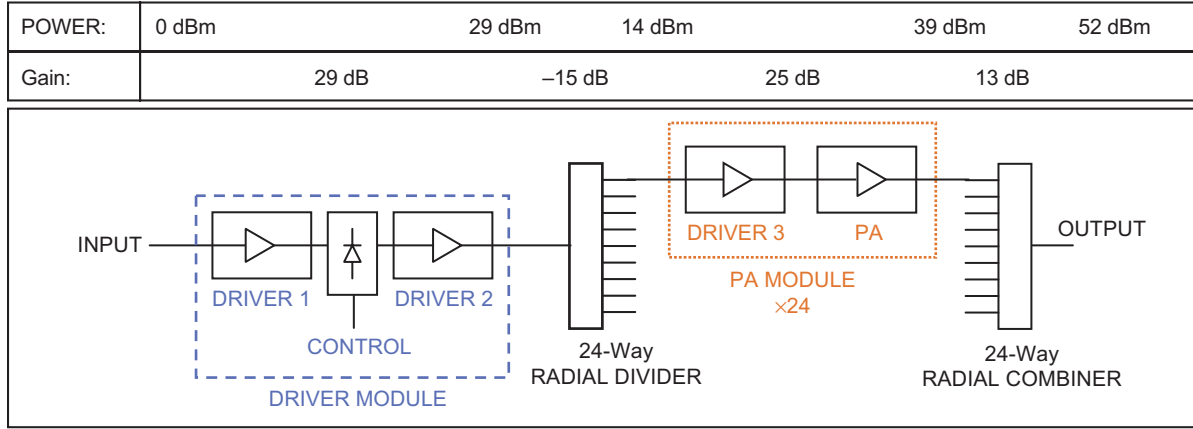


Fig. 12. Physical architecture of an SSPA based on a waveguide radial divider/combiner: (a) a plan view showing the layout of the power combiner and MMIC modules and (b) a cross-section view showing orientation of the input divider, output combiner, and MMIC modules.



**Fig. 13. RF architecture of a 52-dBm SSPA with 52-dB gain based on a 24-way waveguide radial divider and combiner.**

**Table 2. 24-way waveguide radial combiner 160-W (52-dBm) SSPA estimates.**

Parameter	Value
Order of combining	$N = 24$
Power combiner loss	0.25 dB
Total combining loss, including MMIC package and transition	0.8 dB (83 percent combining efficiency)
Prototype mass	4.4 kg
Prototype volume	$\sim 2350 \text{ cm}^3$
Required MMIC power	8 W
Required MMIC PAE	48 percent

The HFSS analysis results for the combiner are illustrated in Fig. 14. Due to processing speed and memory limitations, the combiner cannot be analyzed as a whole. Instead, a sector of the combiner containing two input ports, indicated by dashed red lines in Fig. 14, was simulated in HFSS with appropriate boundary conditions. (A similar technique was successfully employed to analyze the base of the waveguide radial combiner discussed previously.) Thus, only the isolation between two adjacent ports was obtained through the analysis. However, it is expected that this represents the worst case and that the isolation between non-neighboring ports will be greater.

Very good performance was achieved over the 31- to 36-GHz band. The input match is better than 24 dB, the output match is better than 22 dB, and the adjacent-port isolation is better than 20 dB over this band. The insertion loss to the coaxial port is calculated to be less than 0.08 dB. This includes the conductor loss of electro-deposited gold ( $3.3 \times 10^7 \text{ S/m}$ ). HFSS analysis also indicates that a coaxial-to-waveguide adaptor, if included at the output, would add an additional 0.07 dB to the insertion loss. If we also include the loss of a 10-cm-long input waveguide (0.08 dB), which is likely to be required by the SSPA layout, the total loss of the combiner, from waveguide input to waveguide output, is expected to be less than 0.23 dB.

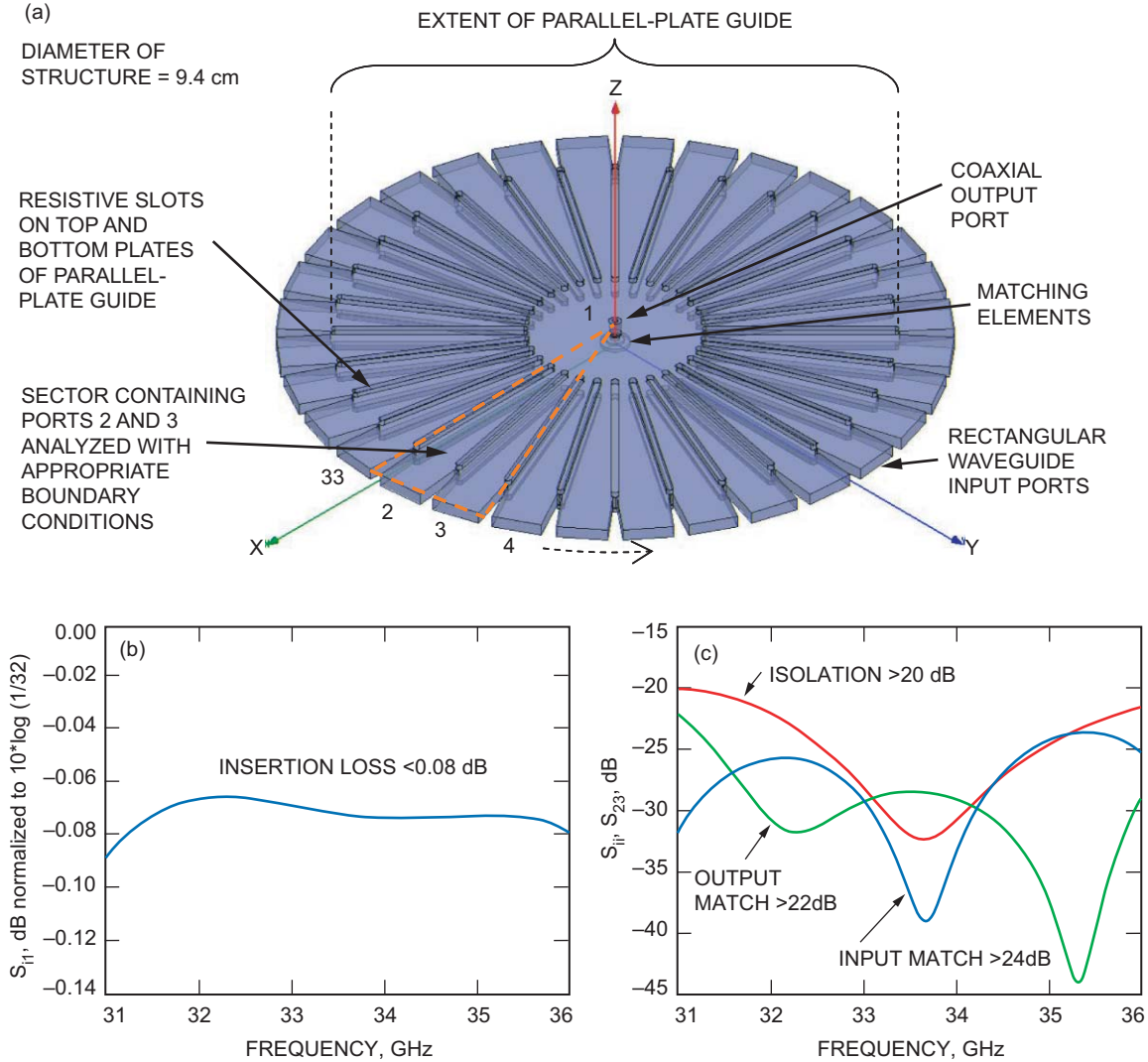


**Fig. 14.** HFSS analysis of a 32-way parallel-plate radial combiner design with waveguide inputs: (a) geometry of the 32-way parallel-plate radial combiner, (b)  $S_{i1}$  (relates to insertion loss) at port  $i$  due to the coaxial port (port 1), and (c)  $S_{ii}$ , the input match at each rectangular port and the coaxial port and  $S_{23}$ , the coupling between adjacent rectangular waveguide ports.

**2. 32-Way Parallel-Plate Combiner SSPA Architecture.** The physical architecture of the parallel-plate combiner-based SSPA is illustrated in Fig. 15. As in the previous two architectures, the driver and the PA modules are mounted directly on the baseplate for efficient heat removal. As illustrated in the cross-section view, the combiner and divider are oriented back-to-back. This allows the input signal to be coupled from the bottom using a coaxial line and the output signal to be coupled through the waveguide on top. As illustrated in the plan view, the narrow diameter of the input coaxial line allows it to be routed between two sets of radial waveguide runs.

As in the waveguide radial combiner SSPA, the diameter of this structure is driven by the width of the MMIC modules. The indicated 32-cm-diameter corresponds to full-width modules that can accommodate a standard WR-28 flange. If a non-standard flange is used and if thermal considerations allow, the diameter of the SSPA can be significantly reduced by decreasing the module width.

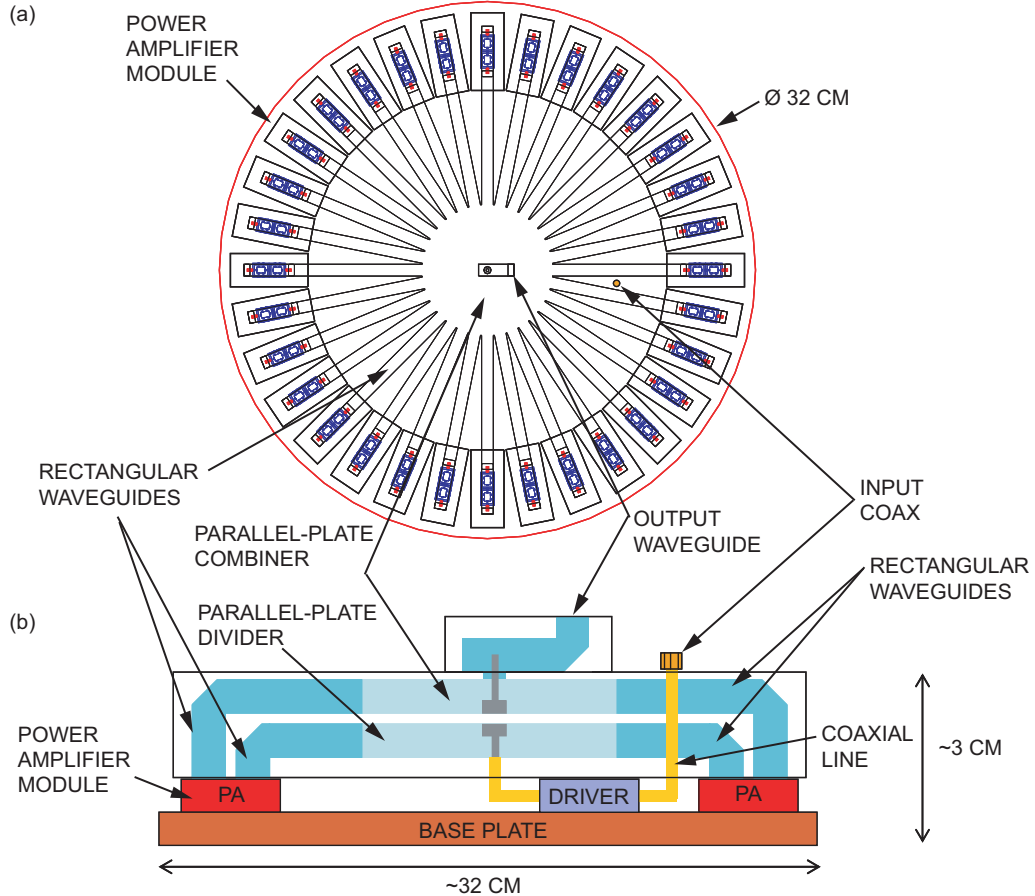


**Fig. 15. Physical architecture of an SSPA based on a parallel-plate divider and combiner:** (a) a plan view showing the layout of the power combiner and MMIC modules and (b) a cross-section view showing the orientation of the input divider, output combiner, and MMIC modules.

The RF architecture of the parallel-plate combiner-based SSPA is illustrated in Fig. 16. Thirty-two PA modules are power combined to deliver a 52-dBm output. For the purpose of calculating the power and gain of each block, the losses of the divider and combiner circuit were assumed to be 1 dB each. A driver MMIC with sufficient gain is included in the PA module to deliver a PA module gain of 25 dB. The driver module, housing two driver MMICs and control circuits, would need to deliver 29-dBm drive power with 29-dB gain.

**3. 32-Way Parallel-Plate Radial-Combiner SSPA Performance Estimates.** In summary, the performance estimates for a 160-W SSPA based on a 32-way parallel-plate radial combiner are given in Table 3.

### III. Conclusion

Results of this article indicate that architectures based on at least three power combiner designs are likely to enable the target of a 120-W, 40 percent PAE SSPA. Each of the three architectures studied can power combine with >80 percent combining efficiency. The required number of MMICs is different for each architecture; the required number of individual MMICs ranges from 16 to 32. This range translates to a MMIC requirement of 5- to 10-W output power and >48 percent PAE.

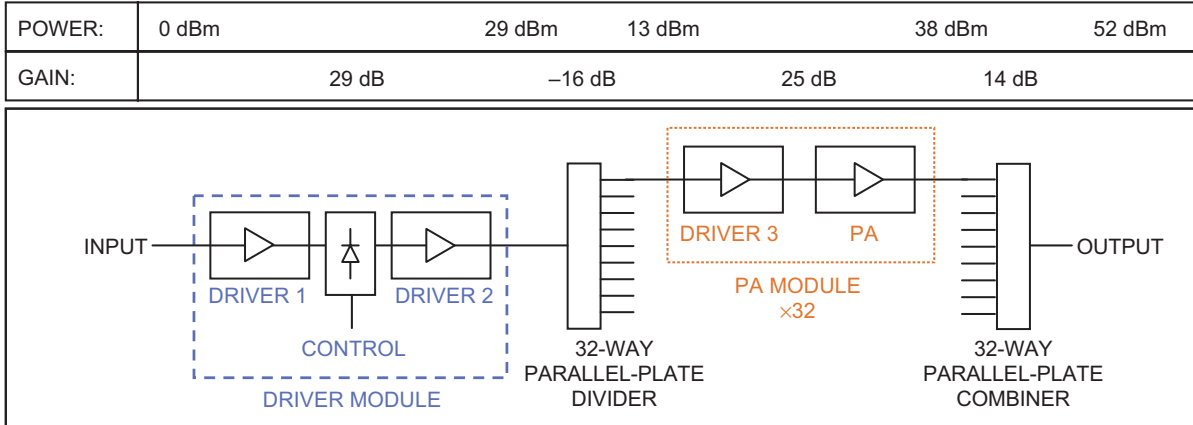


**Fig. 16.** RF architecture of a 52-dBm output, 52-dB gain SSPA based on a parallel-plate divider and combiner.

**Table 3. 32-way parallel-plate radial combiner 160-W (52-dBm) SSPA estimates.**

Parameter	Value
Order of combining	$N = 32$
Combiner loss	0.23 dB
Total combining loss, including MMIC package and transition	0.8 dB (83 percent combining efficiency)
Prototype mass	4.6 kg
Prototype volume	$\sim 2400 \text{ cm}^3$
Required MMIC power	6 W
Required MMIC PAE	48 percent

The first architecture studied is a 16-way septum combiner with low loss and high isolation. Simulated performance of a single combiner predicts that it will exceed the required design bandwidth of 31 to 36 GHz. The simulation of the 2-way septum combiner had an input match  $>25$  dB, output match  $>30$  dB, insertion loss  $<0.02$  dB, and isolation  $>30$  dB from 31 to 36 GHz. The 16-way combiner would cascade the simulated combiner in a binary fashion.

The second architecture is based on a 24-way waveguide radial combiner. A prototype 24-way radial base was analyzed to have an input match  $>30$  dB (under equal excitation of all input ports). A mode transducer was designed with a match of  $>27$  dB. The mode transducer in combination with the radial base will function as a radial combiner/divider. The analyses of the radial base and mode transducer meet the required bandwidth of the radial combiner. Measurements of the radial base, the mode transducer, and the radial combiner/divider are planned.

The third architecture employs a 32-way, parallel-plate radial combiner. Simulation results indicated an input match  $>24$  dB, output match  $>22$  dB, insertion loss  $<0.23$  dB, and adjacent port isolation  $>20$  dB over the design band.

All three architectures utilize a low-loss MMIC amplifier module based on commercial MMIC packaging and a custom microstrip-to-rectangular waveguide transition. The insertion loss of the module is expected to be 0.45 dB over the design band.

## Acknowledgments

The authors would like to acknowledge the following individuals for making significant contributions to the work documented in this article: Daniel J. Hoppe, JPL, and Dan Kelley, Honeywell Technology Solutions, Inc.

## References

- [1] P. Khan, L. Epp, and A. Silva, "Ka-Band Wide-Bandgap Solid-State Power Amplifier: Architecture Identification," *The Interplanetary Network Progress Report*, vol. 42-162, Jet Propulsion Laboratory, Pasadena, California, pp. 1–16, August 15, 2005. [http://ipnpr.jpl.nasa.gov/progress\\_report/42-162/162E.pdf](http://ipnpr.jpl.nasa.gov/progress_report/42-162/162E.pdf)
- [2] P. Khan, L. Epp, and A. Silva, "Ka-Band Wide-Bandgap Solid-State Power Amplifier: General Architecture Considerations," *The Interplanetary Network Progress Report*, vol. 42-162, Jet Propulsion Laboratory, Pasadena, California, pp. 1–19, August 15, 2005. [http://ipnpr.jpl.nasa.gov/progress\\_report/42-162/162F.pdf](http://ipnpr.jpl.nasa.gov/progress_report/42-162/162F.pdf)
- [3] G. Chattopadhyay and J. Carlstrom, "Finline Ortho-Mode Transducer for Millimeter Waves," *IEEE Microwave and Guided Wave Letters*, vol. 9, pp. 339–341, September 1999.
- [4] F. Takeda, O. Ishida, and Y. Isoda, "Waveguide Power Divider Using Metallic Septum with Resistive Coupling Slot," *IEEE MTT-S Int. Microwave Symposium*, pp. 527–528, June 1982.
- [5] A. R. Khan, L. W. Epp, D. J. Hoppe, and D. Kelley, *Thin-Film Resistive Septum Waveguide Power Combiner*, provisional patent application no. 48,467, docket number CIT-4300-P, filed January 21, 2005.
- [6] E. Marx, "Modeling of a 192-Way Power Divider," Ansoft HFSS Users' Workshop, Los Angeles, California, January 2002.
- [7] L. W. Epp, D. J. Hoppe, A. R. Khan, and D. T. Kelley, *Wideband (31 to 36 GHz) 24-Way Radial Power Combiner/Divider Fed by a Marie Transducer*, provisional patent application, CIT file no. CIT-4336-P, filed March 18, 2005.
- [8] S. S. Saad, J. B. Davies, and O. J. Davies, "Analysis and Design of a Circular TE<sub>01</sub> Mode Transducer," *Microwave, Optics and Acoustics*, vol. 1, pp. 58–62, January 1977.
- [9] A. R. Khan, L. W. Epp, and D. J. Hoppe, *Wideband (31 to 36 GHz) Parallel Plate Power Combiner/Divider with Isolation*, provisional patent application, CIT file no. CIT-4372-P, filed May 3, 2005.
- [10] T.-I. Hsu and M. Simonutti, "A Wideband 60 GHz 16-Way Power Divider Combiner Network," *IEEE MTT-S International Microwave Symposium Digest*, vol. 84, issue 1, pp. 175–177, May 1984.